

# Transverse mode selection in laser resonators using volume Bragg gratings

Brian Anderson<sup>1,\*</sup>, George Venus<sup>1</sup>, Daniel Ott<sup>1</sup>, Ivan Divliansky<sup>1</sup>, Jay W Dawson<sup>2</sup>, Derrek R Drachenberg<sup>2</sup>, Mike J. Messerly<sup>2</sup>, Paul H. Pax<sup>2</sup>, John B. Tassano<sup>2</sup>, Leonid Glebov<sup>1</sup>

<sup>1</sup>CREOL, The College of Optics and Photonics, University of Central Florida, P.O. Box 162700, Orlando, Florida 32816-2700, USA

<sup>2</sup>Lawrence Livermore National Lab, L-491, P.O. Box 808, Livermore, California 94551, USA

## ABSTRACT

Power scaling of high power laser resonators is limited due to several nonlinear effects. Scaling to larger mode areas can offset these effects at the cost of decreased beam quality, limiting the brightness that can be achieved from the multi-mode system. In order to improve the brightness from such multi-mode systems, we present a method of transverse mode selection utilizing volume Bragg gratings (VBGs) as an angular filter, allowing for high beam quality from large mode area laser resonators. An overview of transverse mode selection using VBGs is given, with theoretical models showing the effect of the angular selectivity of transmitting VBGs on the resonator modes. Applications of this ideology to the design of laser resonators, with cavity designs and experimental results presented for three types of multimode solid state lasers: a Nd:YVO<sub>4</sub> laser with 1 cm cavity length and 0.8 mm diameter beam with an  $M^2$  of 1.1, a multimode diode with diffraction limited far field divergence in the slow axis, and a ribbon fiber laser with 13 cores showing  $M^2$  improved from 11.3 to 1.5.

**Keywords:** Volume Bragg grating, PTR, transverse mode selection, beam quality, laser resonator

## 1. INTRODUCTION

Power scaling in laser systems is usually limited to nonlinear effects<sup>1, 2</sup>. Thermal lensing, stimulated Brillouin scattering (SBS), and other limiting nonlinear effects can be mitigated by increasing the mode area, which has the effect of reducing the overall irradiance in the system. To realize this effect, either the aperture or the waveguide dimensions are increased. However, by increasing the limiting aperture or waveguide dimensions, more transverse modes are allowed to oscillate in the resonator, reducing the beam quality and reducing the brightness of the laser. The higher power levels allowed by the increased aperture size are offset by the decreased beam quality, preventing any improvements to the brightness. To fully take advantage of the reduced nonlinearities in multi-mode systems, new transverse mode selection techniques are needed to force the system to operate in the single (usually fundamental) mode.

Many methods of transverse mode selection currently exist and are useful in improving the brightness in laser systems. However, many of these methods rely on the use of an aperture in the far field and increase the cavity size. By using diffractive optical elements, a spatial filter can be holographically recorded into a compact device, allowing for the design compact resonators<sup>3</sup>. In particular, the volume Bragg grating (VBG) is one such device which offers narrow angular selectivity, allowing it to be used as an angular spatial filter. Such devices have previously been demonstrated to produce diffraction limited output from both diode and solid state lasers<sup>4, 5</sup>. In this proceeding, we discuss the theoretical characteristics of the VBG which allow for the design of single transverse mode resonators, and demonstrate three applications to laser design which use the angular selectivity of the VBG to force the multi-mode laser to operate with a single transverse mode and high efficiency.

## 2. VOLUME BRAGG GRATINGS

Volume Bragg gratings are holographically recorded in a photosensitive glass known as photo-thermo-refractive glass (PTR)<sup>6</sup>. Exposure to near UV radiation followed by thermal development results in refractive index changes up to 1000 ppm ( $\delta n$  is about  $10^{-3}$ ).

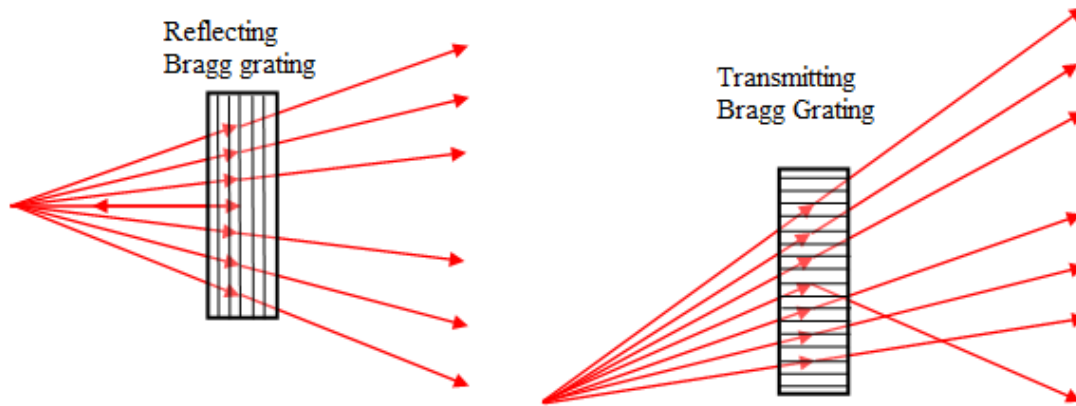


Figure 1: Illustration of orientation of volume gratings and the types of VBGs. For a divergent beam incident on the grating, the VBG acts as a slit (transmitting grating) or round diaphragm (reflecting grating) in angular space, diffracting only a small portion of the light.

Theoretical modeling of volume Bragg gratings has been analytically described by Kogelnik<sup>7</sup>, by way of coupled-wave theory. This theory accurately predicts the diffraction efficiency of a plane wave incident on a sinusoidal modulated hologram. Small angular deviations from the Bragg condition show a drop off in diffraction efficiency. Based on the orientation of the grating within the glass, the VBG falls into two distinct categories. With the grating vector oriented near normal to the surface of the glass, the VBG reflects light backwards (reflecting Bragg gratings, RBG, Bragg mirror). While a grating vector oriented near parallel to the surface will transmit light through the glass (transmitting Bragg grating, TBG). An example of the types of VBGs is shown in Figure 1.

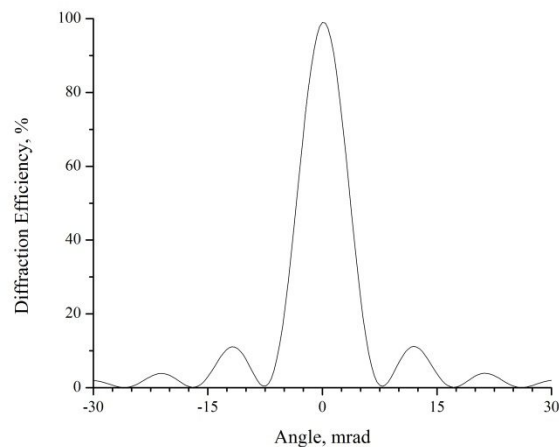


Figure 2: Measured diffraction efficiency for a TBG with 7.1 mrad FWHM, 99.0% peak diffraction efficiency and a thickness of 1.0 mm.

For a transmitting Bragg grating oriented  $90^\circ$  to the normal of the surface, the ratio of the scattered amplitude to the incident amplitude ( $S$ ) is given as function of the dephasing ( $\xi$ ) from the Bragg condition and the grating strength ( $\nu$ ) (Eq. 1). The diffraction efficiency for a plane wave is therefore the amplitude squared of  $S$ . The dephasing term (Eq. 2) shows the change in the diffraction efficiency as the incident plane wave makes small deviations from the Bragg condition, and is a function of the Bragg period ( $\Lambda_B$ ), the angular deviation ( $\delta\theta$ ) from the Bragg angle ( $\theta_B$ ) in the medium, and the thickness of the grating ( $d$ ). The grating strength (Eq. 3) controls the maximum diffraction efficiency, and is a function of the peak to peak refractive index modulation ( $\delta n$ ), the grating thickness, the wavelength ( $\lambda$ ) in the medium, and the Bragg angle in the medium. For a grating strength of  $\nu = \pi$ , the diffraction efficiency is 100%.

$$S = -ie^{-i\xi d} \left( \frac{\sin(\sqrt{\xi^2 + \nu^2})}{\sqrt{1 + \frac{\xi^2}{\nu^2}}} \right) \quad (1)$$

$$\xi = \frac{2\pi}{\Lambda_B} \delta\theta d \quad (2)$$

$$\nu = \frac{\pi\delta n}{\lambda \cos(\theta_B)} \quad (3)$$

An example of the diffraction efficiency as a function of detuning from the Bragg condition is plotted in Figure 2. For this TBG, the maximum diffraction efficiency is 99.0%, and the FWHM of the angular selectivity in air is 7.1 mrad. These two parameters are the most important for determining the effect a TBG will have on an incident beam. The peak diffraction efficiency determines the maximum amount of power that will be diffracted by the grating for a plane wave. For a finite beam, such as a Hermite-Gaussian transverse mode or LP mode, the angular selectivity determines what percentage of the angular content of the beam will be diffracted by the grating.

It was shown that diffraction for arbitrary, near collimated, wave fronts can be described by a convolution between Kogelnik's plane wave solution and the spatial distribution of the electric field for an arbitrary wave front<sup>8, 9</sup>. These theories allow for the description of the diffraction efficiency of a VBG interacting with the Hermite-Gaussian modes of a stable resonator, or the LP modes of a circular core fiber, and have been used to theoretically model the performance of VBGs in PTR interacting with Gaussian beams<sup>5, 9</sup>. The formulation of the plane-wave decomposition is:

$$E_{diff}(x, y, d) = \int_{-\infty}^{\infty} \int_{-\infty}^{\infty} E(k_x, k_y) S_{TBG} e^{-i(xk_x + yk_y + d\sqrt{1-k_x^2-k_y^2})} dk_x dk_y \quad (4)$$

$$E(k_x, k_y) = \int_{-\infty}^{\infty} \int_{-\infty}^{\infty} E(x, y, 0) e^{i(xk_x + yk_y)} dx dy \quad (5)$$

$$E(x, y, 0) = E_0 H_n \left( \frac{\sqrt{2}x}{w_{x,0}} \right) e^{-\frac{x^2}{w_{x,0}}} H_m \left( \frac{\sqrt{2}y}{w_{y,0}} \right) e^{-\frac{y^2}{w_{y,0}}} \quad (6)$$

To understand the effect the TBG has on finite beams, and specifically the Hermite-Gaussian modes, modeling was done using the previously mentioned formalism. Using the Hermite-Gaussian modes, the diffraction efficiency was calculated as a function of the FWHM angular selectivity of the grating normalized to the  $1/e^2$  diameter (FWE<sup>2</sup>M) of the fundamental Gaussian mode. The grating modeled had a plane wave diffraction efficiency of 100%, and the thickness was kept constant at 1.0 mm while the Bragg period was modified to change the angular selectivity. Diffraction efficiencies were calculated for the first 3 modes ( $n = 0, 1, 2$  &  $m=0$ ) and are plotted in Figure 3. The divergence of the fundamental mode can be estimated using the well-known relation  $\theta = \lambda/(\pi w_0)$ , while the angular acceptance of the grating is proportional to the Bragg period. From Figure 3, it is clear that the higher order modes diffracted by TBGs always have larger losses compared to the fundamental mode. When the fundamental mode is equal to the angular selectivity of the grating, the diffraction efficiency for the fundamental mode is approximately 80% while the TEM<sub>10</sub> mode experiences 40% diffraction efficiency. Increasing the angular acceptance of the TBG increases the diffraction efficiency of the fundamental mode, and when the angular acceptance is approximately 5 times the far field divergence, the diffraction efficiency is increased to 99%, while the TEM<sub>10</sub> mode has 98% diffraction efficiency and the TEM<sub>20</sub> mode has 97% diffraction efficiency. A typical resonator might use a grating with angular selectivity near 2 times the divergence of the fundamental mode, where diffraction efficiency is 96% for the TEM<sub>00</sub> and 88% for the TEM<sub>10</sub>. Although such losses might be insufficient for complete spatial filtering of a beam in a free space setup, in a resonator such losses can be sufficient to suppress all but the fundamental order mode.

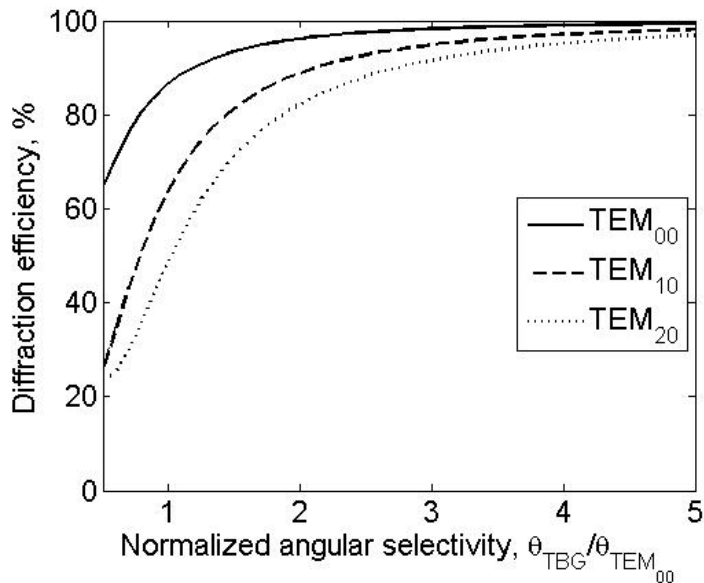


Figure 3: Diffraction efficiency for the first three Hermite-Gaussian modes as a function of angular selectivity of the TBG (FWHM) normalized to the far field divergence of the TEM<sub>00</sub> mode (FW $e^{-2}M$ ).

### 3. LASER DESIGN

#### 3.1 Solid State Lasers

Design of single transverse mode solid state resonators is a two part problem to ensure that both the aperture size is small enough to limit the angular content of the beam to only the fundamental mode, and secondly to ensure the fundamental mode is of comparable size relative to the aperture to ensure maximum energy extraction. As a rule of thumb, the Fresnel number  $N$  of the cavity must be approximately 1 to ensure the angular content of the beam is limited to only the fundamental mode:

$$N = \frac{a^2}{\lambda L} \quad (7)$$

where  $a$  is the radius of the limiting aperture of the cavity,  $L$  is the cavity length, and  $\lambda$  is the wavelength of the system. Satisfaction of this rule could be a difficult problem, especially in the case of compact laser systems. Systems at a wavelength of 1  $\mu\text{m}$  with a cavity length below 1 cm require an aperture size smaller than 100  $\mu\text{m}$ .

As previously mentioned, this requirement on the length of the cavity is only necessary to reduce the angular content of the oscillating wave within the resonator, and if the angular content could be filtered through other means, the cavity could be single mode in a significantly more compact resonator, while using a larger aperture size. Using a 7.1 mrad TBG as the angular filter, a 1 cm long cavity was designed (Figure 4)<sup>5</sup>. Due to the asymmetry of the TBG (narrow angular selectivity occurs mainly in the plane of diffraction), two gratings were needed to produce a circularly symmetric beam.

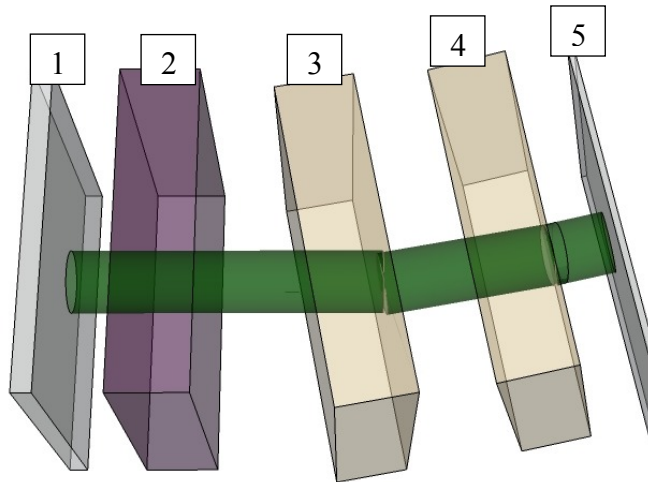


Figure 4: Design of a 1 cm long planar cavity<sup>5</sup>. 1) high reflective dichroic, allowing for 808 nm pump to be transmitted and 1064 nm signal to be reflected with >99% reflectivity, 2) 1 mm thick slab of a-cut 1% At. Nd:YVO<sub>4</sub>, absorbs >70% of the partially polarized pump, 3) 7.1 mrad TBG aligned to diffract along the horizontal plane, 4) 7.1 mrad TBG aligned to diffract in the vertical plane, 5) 80% reflective output coupler.

For the planar cavity design shown in Figure 4, using a 0.8 mm diameter pump beam and a 7.1 mrad TBG, generation was produced with an  $M^2$  of 1.2 and a slope efficiency of 30%. While slope efficiency was reduced relative to the multi-mode efficiency, it is worth noting that such a system could not be realized using a standard aperture. In the 1 cm long cavity, an aperture of approximately 100  $\mu\text{m}$  would be required, which would block all but 94% of the pump light and corresponding drop of emitting power. It is clear, that in this compact cavity, the TBG allows a larger mode area to be used compared to what could be achieved using an aperture.

### 3.2 Diode

Power output from a single mode emitter is limited due to several nonlinear effects, meaning that multi-mode diodes are necessary to achieve higher power levels. However, even the output power from a single multi-mode emitter is limited to the level of some tens of watts. To further improve the brightness from a single emitter, transverse mode selection techniques are needed.

In slab waveguide lasers, such as wide-stripe diodes, the output beam is typically astigmatic, with the fast axis near single mode with diffraction limited divergence, while the slow axis is typically multi-mode, with the number of modes related to the width of the stripe. The different modes of the slow axis experience different gain and losses depending on the overlap with the gain. For typical diodes the higher order modes have a better overlap with the gain, meaning the output intensity typically has a much larger fraction comprised of these higher order modes, causing the intensity to form a two lobed pattern in the far field (Figure 5).[4] Due to the lower losses of these modes, any mode selection techniques will operate with much higher efficiency if they can force the laser to operate in a pure higher order mode.

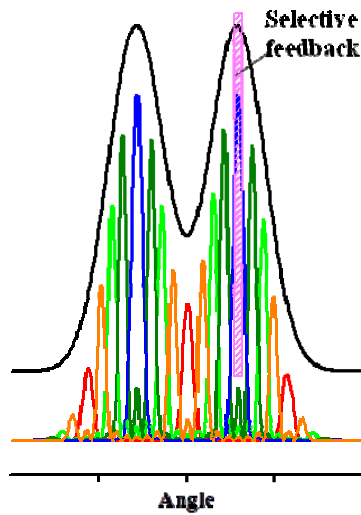


Figure 5: Typical intensity pattern from a multi-mode diode<sup>4</sup>. Strong preference is seen for the higher order modes, causing the intensity to produce a two-lobed pattern.

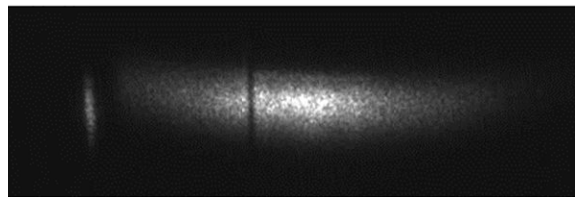


Figure 6: Image of ASE with TBG diffracting a narrow angular portion of the beam<sup>4</sup>. The TBG is not aligned to the central portion of the beam, so that it can provide selective feedback for a higher order mode.

As shown in the solid state laser, the TBG can act as a slit in angular space, forcing the oscillating radiation to be confined within the angular acceptance of the grating. By rotating the TBG slightly, selective feedback can be provided for one of the higher order modes (Figure 5, 6). Such a system can be realized as a compact resonator (Figure 7). Such a resonator was constructed<sup>4</sup>, and found to operate with slope efficiency of 0.902 W/A, a value which was 98.9% of the multi-mode resonator. Furthermore, the far field beam divergence was found to be drastically reduced to 0.62° (Figure 8), indicating a >10 improvement in spatial brightness.

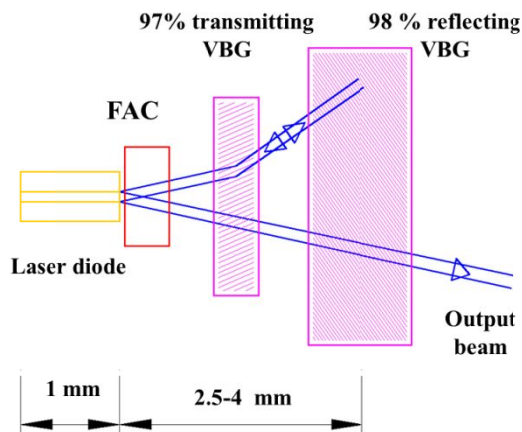


Figure 7: Diagram of TBG mode selective cavity<sup>4</sup>. The TBG diffracts one lobe of a higher order mode, while the RBG provides feedback for that mode. The other lobe of the higher order mode does not interact with either grating and exits the cavity.

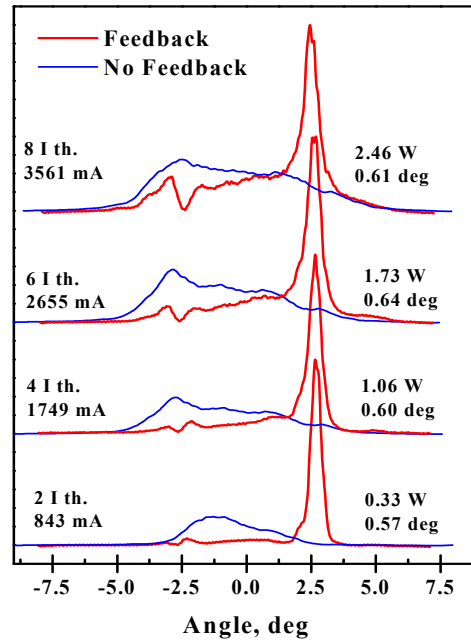


Figure 8: Diagram of far field beam divergence for the cavity shown in figure 3<sup>4</sup>. Beam divergence is reduced to 0.62° with a 1% decrease in output power, indicating a large improvement in brightness.

### 3.3 Fiber

As with power scaling in diodes, increasing the area of the active core is the easiest means of achieving higher output powers. However, modeling has shown that while aperture size can increase the available output power to beyond the stimulated Brillouin scattering or stimulated Raman scattering limits, the fiber will still be limited to the power level of 30 KW or so due to the onset of thermal lensing<sup>2</sup>. In order to achieve power levels beyond this level, new fiber designs are needed which can have efficient heat extraction so as to remove the thermal lensing, while maintaining a large core area so as to not be limited by SBS or SRS. A slab like fiber, or ribbon fiber, has been proposed as one such solution. The fiber core has rectangular dimensions, and is multi-mode along the slow axis and single-mode along the fast axis (Fig. 9). Such a fiber can have a large mode area, while maintaining a flat profile which allows for efficient heat extraction, permitting power scaling to high power levels.

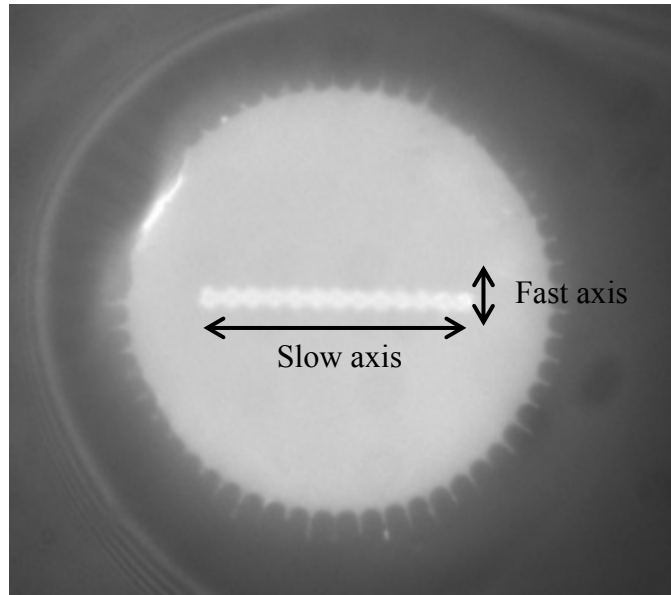


Figure 9: Microscopic image of the ribbon fiber with the core illuminated. The core dimensions are approximately  $108.3\ \mu\text{m}$  by  $8.3\ \mu\text{m}$ .

The fiber used in this experiment was fabricated via a photonic crystal stack and draw process. Thirteen ytterbium-doped silica rods were stacked within a larger stack of un-doped silica rods to form a raised index ribbon core visible in Figure 9. The Yb-doped silica rods were fabricated by Heraeus Tenevo; they are co-doped with 0.05 mol. %  $\text{Yb}_2\text{O}_3$ , and 1.0 mol. %  $\text{Al}_2\text{O}_3$ , with the manufacturer's goal of 250 dB/m absorption at 976 nm. The Yb-doped silica had a refractive index of  $2.54 \times 10^{-3}$  above that of the pure silica giving a core NA of 0.086. The pump cladding was formed with a single circular row of silica capillaries which were expanded with a few kPa of air during the draw to form a 0.3 NA air-cladding. The core is approximately  $8.3 \times 107.8\ \mu\text{m}$ , while the air cladding has an inner diameter of  $167\ \mu\text{m}$ . The fiber's outer dimension is  $245\ \mu\text{m}$ .

Using a 4% output coupler, a 1.0 m section of this fiber was used to construct a multi-mode resonator in order to characterize the fiber. Using a 976 nm pump source, a maximum coupling efficiency of 92% was measured as well as a maximum absorption efficiency of 47%. The multi-mode performance of this fiber was characterized to have an absorbed slope efficiency of 76%, producing a maximum output power of 17.3 W with 23.9 W of absorbed pump. For this output power, the  $M^2$  of the wide axis was 11.3 and for the short axis the  $M^2$  was 1.6. Due to the poor  $M^2$ , the brightness of the system was  $878\ \text{KW}/(\text{mm}^2\ \text{sr})$ .

To improve the brightness of the system, a resonator was designed using a TBG as a mode selecting element (Figure 10). For this first iteration, a TBG was not designed to match the angular content of the fundamental mode, and as such required the use of magnifying optics to properly match the mode size. Future iterations could remove these optics, which could further improve the efficiency and reduce the complexity. Experimental measurements determined that optimal results were produced using a 4.7 mrad TBG with 98% diffraction efficiency, along with 6.67x magnification optics.

In the single-mode resonator (Figure 10), the beam quality and slope efficiency was measured. The  $M^2$  of the multi-mode axis was measured to be 1.45, demonstrating an improvement by a factor of 7.8 over the multi-mode resonator. The far field beam at maximum output power is shown in Figure 11, demonstrating a near Gaussian appearance. No change in beam quality was measured throughout the pump-limited measured range of operation. The slope efficiency of the single-mode system was measured, and a reduction in the output power was seen (Figure 12). In the single mode case, the slope efficiency was reduced to 54% and produced a maximum output power of 11.3 W for an absorbed pump power of 23.7 W, indicating the TBG is adding additional losses to the system. However, despite the additional losses, brightness was improved to  $4450\ \text{kW}/(\text{mm}^2\ \text{sr})$ , indicating a 5.1 times improvement in the brightness over the multi-mode resonator.

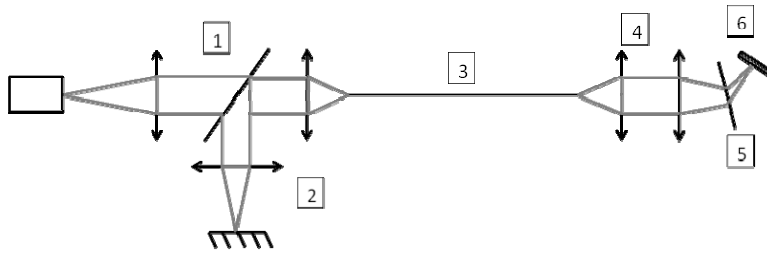


Figure 10: Diagram of the single-mode resonator using the ribbon fiber. (1) A 976 nm pump source is transmitted through the pump combining optics, (2) the signal is reflected on a 100% reflective feedback mirror, (3) 1.0 m section of Yb-doped ribbon fiber, (4) re-imaging optics to match the fundamental mode with the angular selectivity of the TBG, (5) 4.7 mrad TBG with 98% diffraction efficiency aligned to select the fundamental mode of the fiber, (6) 4% reflective output coupler.

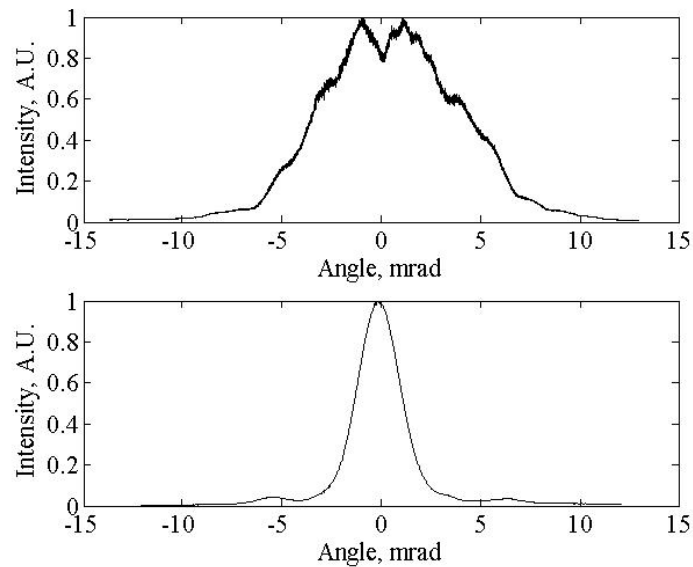


Figure 11: Far field intensity distribution of the (a) multi-mode resonator and (b) single-mode resonator, demonstrating that the narrow angular selectivity can select the fundamental mode of multi-mode fiber lasers.

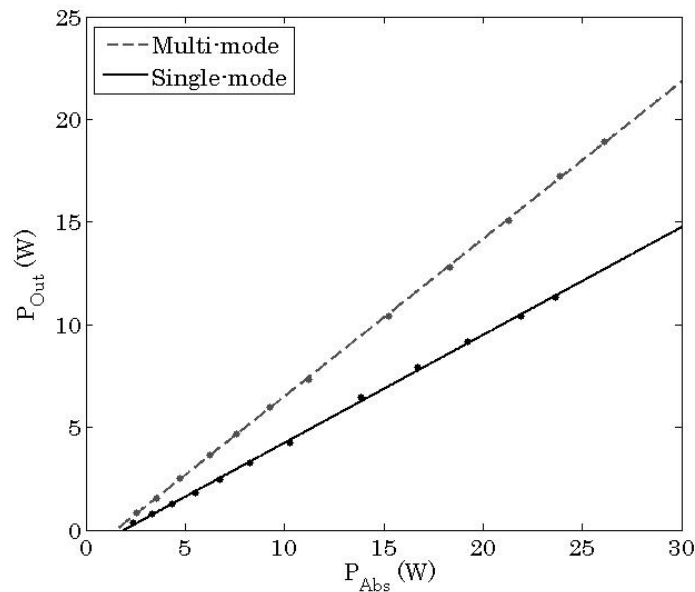


Figure 12: Output power of the multi-mode resonator compared to the single-mode resonator. The TBG adds additional losses to the system, but still can improve the brightness by a factor of 5.1

#### 4. CONCLUSION

In conclusion, we have shown the effects the narrow angular selectivity of a VBG has on both the modes of a bulk stable resonator and the guided modes of a waveguide. We have presented several methods of using the TBG in a resonator to improve the beam quality and brightness of the laser. Although an aperture can achieve a similar spatial filtering effect, such a resonator design requires the aperture to be in the far field of the beam, placing a serious restriction on either the length of the system or generating a high irradiance from a focused beam. Using the spatial filtering of the VBG allows the beam to be angularly filtered entirely within the volume of the grating, allowing for the design of compact systems with large mode areas and high beam quality. We have shown that these methods are applicable to both stable solid state cavities, and to waveguide lasers (diodes, fiber) with external cavities. In a diode laser with many more modes oscillating in the slow axis, diffraction limited output could be seen with only a 1% reduction in performance, showing the brightness improved by a factor of over 10. In a ribbon fiber with approximately 13 modes oscillating in the multi-mode axis, an  $M^2$  of 1.45 was produced with a slope efficiency of 54% and a pump limited output power of 11 W, realizing a brightness improvement of 5.1 times. These experiments show that traditionally multi-mode lasers can be designed to have single-mode output which has important implications for power scaling in large mode area fibers.

#### REFERENCES

- [1] Richardson, D. J., Nilsson, J., and Clarkson, W. A., "High power fiber lasers: current status and future perspectives," *J. Opt. Soc. Am. B* 27, B63 (2010).
- [2] Dawson, J. W., Messerly, M. J., Beach, R. J., Shverdin, M. Y., Stappaerts, E. A., Sridharan, A. K., Pax, P. H., Heebner, J. E., Siders, C. W., and Barty, C. P. J., "Analysis of the scalability of diffraction-limited fiber lasers and amplifiers to high average power.," *Opt. Express* 16, 13240–13266 (2008).
- [3] J.-F. Bisson, N. Lyndin, K. Ueda, and O. Parriaux, "Enhancement of the Mode Area and Modal Discrimination of Microchip Lasers Using Angularly Selective Mirrors," *IEEE J. Quantum Electron.*, vol. 44, no. 7, pp. 628–637, Jul. 2008.

- [4] Venus, G.B., Glebov, L.B., Rotar, V., Smirnov, V., Crump, P., and Farmer, J. "Volume Bragg semiconductor lasers with near diffraction limited divergence," Proc. SPIE 6216, Laser Source and System Technology for Defense and Security II, 621602 (2006).
- [5] Anderson, B., Venus, G., Ott, D., Divliansky, I., and Glebov, L. B., "Compact cavity design in solid state resonators by way of volume Bragg gratings." Proc. SPIE 8959, 89591H (2014).
- [6] Glebov, L. "Photosensitive glass for phase hologram recording," Glass Sci. Technol. 71, 85-90 (1998).
- [7] Kogelnik, H. "Coupled wave theory for thick hologram gratings," Bell Syst. Tech. J. 48, 2909-2947 (1969).
- [8] Hsieh, H., Liu, W., Havermeyer, F., Moser, C., Psaltis, D., "Beam-width-dependent filtering properties of strong holographic gratings," Appl. Opt. 45, 3774-3780 (2006).
- [9] Hellstrom, J. E., Jacobsson, B., Pasiskevicius, V., Laurell, F., "Finite beams in reflecting volume Bragg gratings: Theory and Experiments," IEEE J. Quantum Electron. 44, 81-89 (2008).